An *Ab Initio* MO Calculation for the Bonding Structure of $[Ni(CN)_4]^{2-}$

Mitsuru SANO,* Hiroshi KASHIWAGI,† and Hideo YAMATERA††

Laboratory of Inorganic Chemistry, Faculty of General Education, Nagoya University, Chikusa-ku, Nagoya 464

†*Institute for Molecular Science, Myodaiji, Okazaki 444*

††*Department of Chemistry, Faculty of Science, Nagoya University, Chikusa-ku, Nagoya 464*

(Received June 12, 1981)

An ab initio MO calculation of $[Ni(CN)_4]^{2-}$ has been carried out with a double zeta basis set. The nickel-cyanide interactions are discussed and the electronic change occurring on the coordination of CN^- to Ni^{2+} is shown by using the MO contours and the electron-density difference map. The map shows σ donation from the cyanide orbitals and π back-donation from the metal d_{xy} orbital.

The tetracyanonickelate ion, $[Ni(CN)_4]^{2-}$, is one of the simplest square-planner complexes. Its coordinate bonding is of great interest for inorganic chemists because of its fundamental importance for comparison with the bonding in octahedral complexes. Demuynck *et al.*[1-2] have reported an ab initio molecular orbital (MO) calculation of $[Ni(CN)_4]^{2-}$; however, the bonding structure has not been discussed in detail in terms of the orbital mixing and the electron-density difference on coordination. We have reported the electronic structures of the octahedral complexes, $[M(CN)_6]^{3-}$ (M=Cr, Mn, Fe, and Co) and $[Fe(CN)_6]^{4-}$, by means of both the Hartree-Fock and the discrete-variational-Xα molecular orbital calculations.[3-4] In these reports, the metal-cyanide bonding has been discussed for complexes of different metals and of different oxidation states, and the validity of the orbital mixing rule[3,5,6] has been demonstrated for the coordinate bond.

In the present work, an ab initio MO computation of $[Ni(CN)_4]^{2-}$ has been undertaken to clarify (1) the metal-cyanide bonding structure in $[Ni(CN)_4]^{2-}$ and (2) the electronic change occurring on the coordination of CN^- to Ni^{2+}, on the basis of the MO contours and the electron-density maps.

Computation

The calculation was done in the SCF LCAO MO scheme with a basis set of Gaussian functions ([11s, 7p, 5d][7] for the Ni atom and [9s, 5p][8] for the C and N atoms). The 250 Gaussian functions were reduced to 112 contracted functions. The program JAMOL3 used in the present calculation has been written by Kashiwagi *et al.*,[9] who made the integral calculation more tractable by making use of symmetry properties and an integral approximation scheme based on semi-orthogonalized orbitals.[10-11] The threshold value for the degree of overlap was set at 0.001 in the present calculation. The bond lengths were taken as:[1-2]

Ni-C=1.86 Å and C-N=1.15 Å in D_{4h}.

The x and y axes were taken along the coordinate axes. The calculation of the electron density map was carried out by using the program written by Miyoshi *et al.*[12]

Results and Discussion

The calculated orbital energies and the approximate valence-shell MO's are given in Table 1, together with the corresponding energy values given by Demuynck *et al.*[1] The present results for the orbital energies are 0.02—0.05 a.u. lower than the previous ones. However, the order of MO levels is almost the same as that reported by Demuynck *et al.*,[1] except for two reversals of the orders of adjacent levels. The calculated orbital levels are schematically illustrated in Fig. 1, together with those of the free CN^- ion. Table 2 gives the symmetries of orbitals on the D_{4h} point group. Sigma interactions exist in the orbitals of the a_{1g} and b_{1g} types, π interactions in those of the a_{2u}, b_{2g}, and e_g types, and both interactions in the e_u-type orbitals. The CN^- π orbitals of the a_{2g} and b_{2u} types have no interacting metal orbitals. The important orbitals in forming the metal-cyanide bonds are the 3d, 4s, and 4p orbitals of Ni and the 5σ, 1π, and 2π orbitals of CN^-.

Table 1. Symmetries and energies of valence shell MO's

Symmetry	Energy/a.u.		
	Present results	Literature[1]	
$1a_{2g}$	−0.1449	−0.122	1π
$8e_u$	−0.1457	−0.120	1π
$2e_g$	−0.1495	−0.131	1π
$1b_{2u}$	−0.1589	−0.136	1π
$2b_{2g}$	−0.1746	−0.155	1π
3_{a2u}	−0.1821	−0.159	1π
$9a_{1g}$	−0.1923	−0.182	d_{z^2}
$5b_{1g}$	−0.2022	−0.182	5σ
$7e_u$	−0.2136	−0.194	5σ
$8a_{1g}$	−0.2494	−0.231	5σ
$1e_g$	−0.2661	−0.266	d_{zx}, d_{yz}
$4b_{1g}$	−0.3011	−0.262	4σ
$6e_u$	−0.3200	−0.277	4σ
$1b_{2g}$	−0.3371	−0.355	d_{xy}
$7a_{1g}$	−0.4215	−0.378	4σ
$3b_{1g}$	−0.9261	−0.875	3σ
$5e_u$	−0.9268	−0.877	3σ
$6a_{1g}$	−0.9313	−0.879	3σ

The Natures of MO's. We will discuss the natures of MO's and the orbital interactions. Demuynck *et al.*[1-2] reported that the $d_{x^2-y^2}$ and 4p orbitals of the metal are important in the Ni–CN σ bond. However, the mechanism of the orbital interaction has not been reported. Figure 2 shows the important MO wavefunctions which contribute to the Ni–CN bonding; *i.e.* $8a_{1g}$, $9a_{1g}$, and $5b_{1g}$ in the σ system,

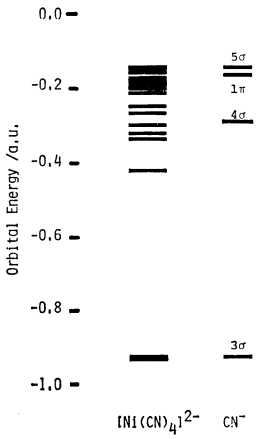

Fig. 1. Schematically illustrated MO energy levels with the levels of free CN^- orbitals.
The MO orderings (from the top to the bottom) are: $1a_{2g}$, $8e_u$, $2e_g$, $1b_{2u}$, $2b_{2g}$, $3a_{2u}$, $9a_{1g}$, $5b_{1g}$, $7e_u$, $8a_{1g}$, $1e_g$, $4b_{1g}$, $6e_u$, $1b_{2g}$, $7a_{1g}$, $3b_{1g}$, $5e_u$, $6a_{1g}$ (See Table 1.).

$1b_{2g}$, $2b_{2g}$, $1e_g$, $2e_g$, and $3a_{2u}$ in the π system, and $7e_u$ and $8e_u$ in the mixed σ and π system. The order of orbital energies in the σ system is $5\sigma<3d\sigma<4s<4p$. In a_{1g} symmetry, two occupied MO's are formed by the combinations of the $5\sigma+3d_{z^2}+4s$ ($8a_{1g}$, Fig. 2a) and $3d_{z^2}-5\sigma-4s$ ($9a_{1g}$, Fig. 2b) types; here the + signs show that the component orbitals have the same sign as that of the main component orbital

Table 2. Symmetry orbitals for D_{4h}

Symmetry	Metal orbital	Cyanide orbital[a)]
a_{1g}	s, d_{z^2}	σ
a_{2g}		π
a_{2u}	p_z	π
b_{1g}	$d_{x^2-y^2}$	σ
b_{2g}	d_{xy}	π
b_{2u}		π
e_g	d_{zx}, d_{yz}	π
e_u	p_x, p_y	σ, π

a) Ligand symmetry orbital.

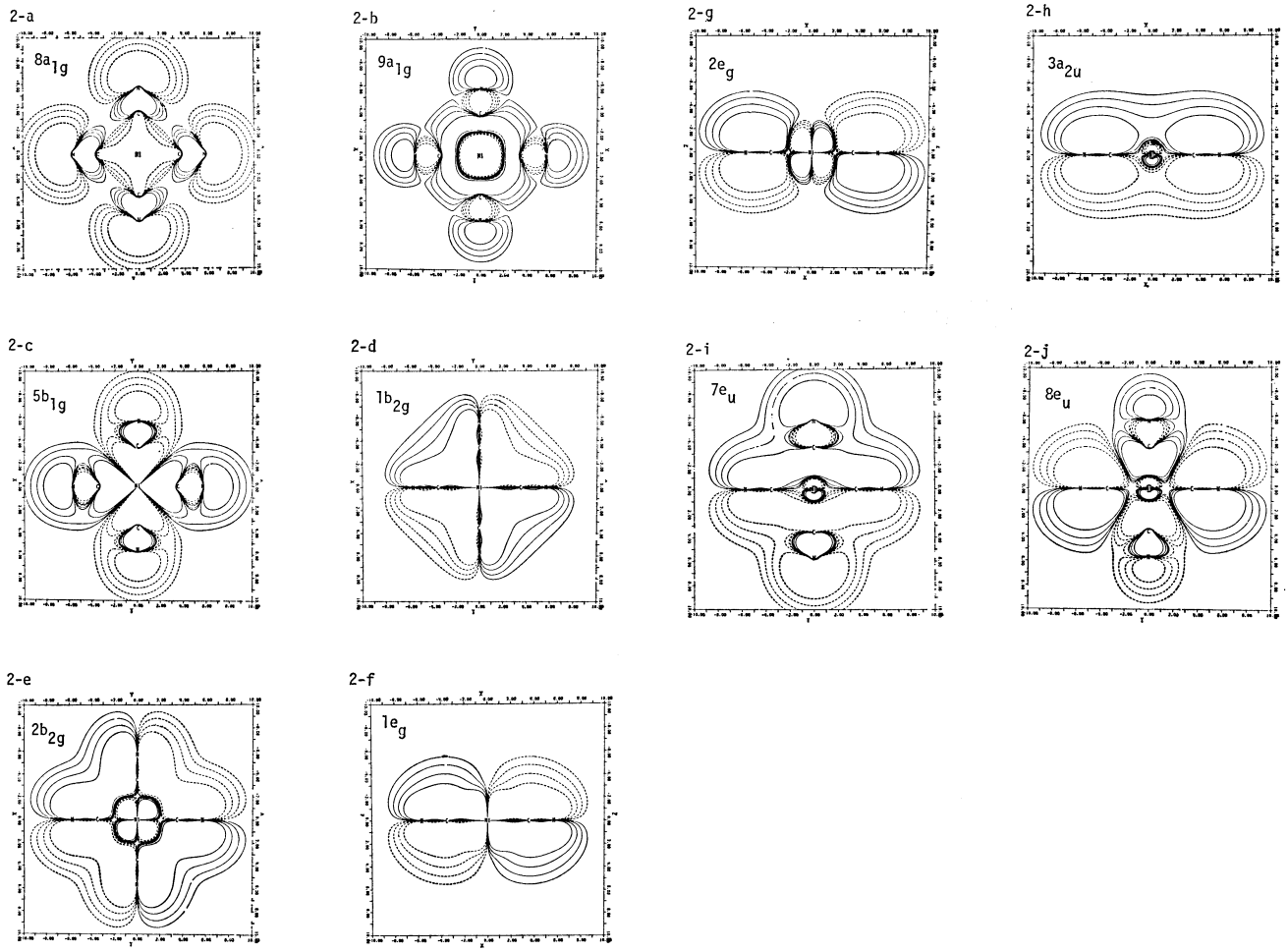

Fig. 2. Selected wavefunction contours for the valence-shell MO's of $[Ni(CN)_4]^{2-}$.
Each set of contours is drawn in a frame of 20 a.u. × 20 a.u. (1 a.u. = 0.529 Å = 52.9 pm). The Ni atom is located at the center of the frame, and four C and four N atoms at the distances of 3.516 a.u. and 5.690 a.u. from the center, respectively, on the xy plane (However, the three figures, f, g, and h, show the wavefunction contours on the xz plane, and two C and two N atoms are located before and behind the Ni atom.). The first solid and dotted contours show ± 0.002, respectively, and neighboring contours differ by a factor of two (For some of the MO's, the signs are reversed.).

(given first) in the region of the Ni–C bonds. If the 4s orbital did not contribute to the two MO's, the linear combinations would be $5\sigma+3d\sigma$ and $3d\sigma-5\sigma$ types; this latter is antibonding and weakens to the Ni–C bonds. This antibonding interaction is relaxed by the mixing of 4s, which thus makes an important contribution to the Ni–CN σ-bond formation. To the b_1 symmetry belongs the occupied $(5\sigma+d_{x^2-y^2})$-type MO ($5b_{1g}$, Fig. 2c), which contributes to the Ni–C bond formation through σ donation.

The order of the energies of π type orbitals is $d\pi<1\pi<4p\pi<2\pi$; $d\pi$ and 1π are originally occupied. The formation of a coordinate bond gives two occupied MO's, $d\pi+1\pi+2\pi$ ($1b_{2g}$, Fig. 2d, and $1e_g$, Fig. 2f) and $1\pi-d\pi-2\pi$ ($2b_{2g}$, Fig. 2e, and $2e_g$, Fig. 2g); the mixing of 2π stabilizes the antibonding $1\pi-d\pi$ MO. In a_{2u}, the $1\pi+4p\pi+2\pi$ combination is formed ($3a_{2u}$, Fig. 2h). The e_u interaction gives the linear combinations $5\sigma+1\pi+4p$ ($7e_u$, Fig. 2i) and $1\pi-5\sigma-4p$ ($8e_u$, Fig. 2j), where the 5σ orbitals of a pair of the CN^- ligands interact with the 1π orbitals of the other pair of the CN^- ligands.

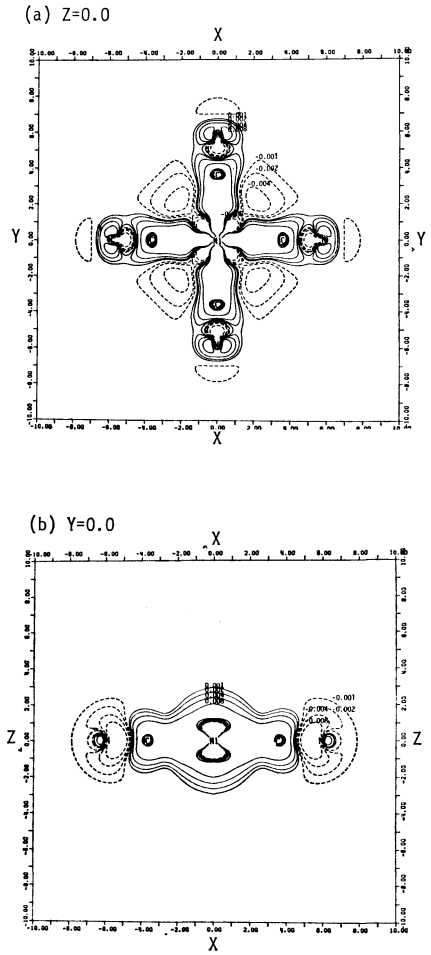

Fig. 3. The electron density difference between $[Ni(CN)_4]^{2-}$ and a cluster of Ni^{2+} (d^8 configuration with unfilled $d_{x^2-y^2}$ orbital) and $(CN^-)_4$: (a) on the xy plane and (b) on the xz plane.
The first solid and dotted contours show ±0.001 e(a.u.)$^{-3}$, respectively, and neighboring contours differ by a factor of two.

As is described above, the interaction of the ligand and the metal occupied orbitals gives rise to two MO's, one with bonding and one with antibonding character; a mixing of the virtual orbitals makes the bonding orbitals more suitable, and the antibonding orbital less unsuitable, to the M–C bonding.

The Electron Density and Population. Figure 3 shows the maps (for the xy and the xz plane) of the electron density difference between $[Ni(CN)_4]^{2-}$ and a system of Ni^{2+} (d^8 configuration with an unfilled $d_{x^2-y^2}$ orbital) and $(CN^-)_4$; the change in the electron density on the formation of the complex is shown in terms of contours. The large positive region between the Ni and C atoms represents a significant σ donation from cyanide to metal. The same feature is also reported by Demuynck *et al.*[2] on the basis of the electron density contours of the localized orbital. The decrease of the electron density in the nickel d_{xy} region results from π back-donation. This π back-donation of d_{xy} increases the nitrogen π_x and π_y populations by the combination of $1\pi-d\pi-2\pi$. This is clearly shown by Fig. 3a. As can be seen from the decrease in the d_{xy} electron density, the extent of π back-donation from d_{xy} is as large as that in $[Fe(CN)_6]^{4-}$ and is larger than that in $[Co(CN)_6]^{3-}$ reported previously.[2,13] There is no indication of the decrease in electron density in the region of d_{zx} (Fig. 3b), suggesting little π back-donation from d_{yz} and d_{zx}. The density increase in the C–Ni–C region and the density decrease in the outer region of CN^- may show the polarization of the coordinated CN^- by the central Ni^{2+} charge and/or the donation of the CN^- electrons to the Ni $3d_{x^2-y^2}$, 4s, and 4p orbitals.

TABLE 3. POPULATION ANALYSIS OF $[Ni(CN)_4]^{2-}$

Orbital	Population (population in free CN^-)		Present results		Literature[1]
Nickel	d_{z^2}		1.935		1.96
	$d_{x^2-y^2}$		0.437		0.91
	d_{xy}		1.956		1.95
	d_{yz}		1.956		1.97
	d_{zx}		1.956		1.97
	4s		0.144		0.52
	$4p_x$, $4p_y$		0.235		0.17
	$4p_z$		0.066		0.07
Atomic charge			+1.533		+0.46
Carbon	2s		1.660	(1.860)	1.26 (1.62)
	$2p\sigma$		1.219	(1.164)	1.14 (1.13)
	$2p\pi_y$	0.801	(1.528)		0.84 (0.84)
	$2p\pi_z$	0.877			0.91 (0.84)
Atomic charge			−0.549	(−0.546)	−0.14 (−0.43)
Nitrogen	2s		1.647	(1.637)	1.66 (1.69)
	$2p\sigma$		1.326	(1.351)	1.53 (1.56)
	$2p\pi_y$	1.222	(2.472)		1.18 (1.16)
	$2p\pi_z$	1.145			1.10 (1.16)
Atomic charge			−0.335	(−0.454)	−0.47 (−0.57)
Bond overlap population					
Ni-C			0.138		
C-N			1.564	(1.666)	

Although the population analysis is to some extent artificial, especially when based on the double-zeta set,[14] the Mulliken populations are given in Table 3 to allow qualitative considerations. (In the free CN^- ion, for example, the listed Mulliken populations are an overestimate for C and an underestimate for N, probably because the wavefunctions are more diffuse for C than for N. However, a comparison of the Mulliken populations before and after the bond formation will give us at least qualitatively reliable information about the nature of the bond, provided that the populations are calculated with the same basis set.) Table 3 also lists the values reported by Demuynck *et al.*[1] They in general agree with our results, but differ in a couple of respects. The Mulliken populations are known to depend on the basis functions; our $d_{x^2-y^2}$ population may thus be an underestimate, probably because one of the components of the split 2p orbital of carbon was too diffuse. Correspondingly, the calculated charge of the nickel atom is higher and that of the carbon atom is lower than the literature values. A significant donation from the C 2s orbital to the Ni $d_{x^2-y^2}$ and 4s orbitals can be seen in Table 3 and also in Fig. 3. The π back-donation from the Ni d_{xy} orbital to the N $2p\pi$ orbitals, which is not found in Table 3, is clearly shown by Fig. 3a, while the small π back-donation from the Ni d_{zx} (and d_{yz}) orbitals to the CN^- $2p\pi_z$ orbitals and the polarization of the latter are demonstrated both by Fig. 3b and by the present and previous results shown in Table 3. The electron-density difference maps are more useful and probably more reliable than the numerical results of the population analysis in discussing the nature of the bonds.

The work was partly supported by the Joint Studies Program (1979—1980) of the Institute for Molecular Science. The computation has been carried out on a HITAC M-180 computer of the Institute for Molecular Science.

References

1) J. Demuynck, A. Veillard, and G. Vinot, *Chem. Phys. Lett.*, **10**, 522 (1971).
2) J. Demuynck and A. Veillard, *Theoret. Chim. Acta*, **28**, 241 (1973).
3) M. Sano, Y. Hatano, H. Kashiwagi, and H. Yamatera, *Bull. Chem. Soc. Jpn.*, **54**, 1523 (1981).
4) M. Sano, H. Adachi, and H. Yamatera, *Bull. Chem. Soc. Jpn.*, **54**, 2898 (1981).
5) S. Inagaki and K. Fukui, *Chem. Lett.*, **1974**, 509.
6) S. Inagaki, H. Fujimoto, and K. Fukui, *J. Am. Chem. Soc.*, **98**, 4054 (1976).
7) B. Roos, A. Veillard, and G. Vinot, *Theoret. Chim. Acta*, **20**, 1 (1971).
8) T. H. Dunning, Jr., *J. Chem. Phys.*, **53**, 2823 (1970).
9) H. Kashiwagi, T. Takada, E. Miyoshi, S. Obara, and F. Sasaki, "Program JAMOL3," Program Library, Computer Center of Institute for Molecular Science.
10) H. Kashiwagi, *Int. J. Quantum Chem.*, **10**, 135 (1976).
11) H. Kashiwagi and T. Takada, *Int. J. Quantum Chem.*, **12** 449 (1977).
12) E. Miyoshi, M. Sano, C. Watanabe, and H. Kashiwagi, "Program JAPICl," Program Library, Computer Center of Institute for Molecular Science.
13) M. Sano, H. Adachi, H. Kashiwagi, and H. Yamatera, The 29th Symposium on Coordination Chemistry of the Chemical Society of Japan, Hamamatsu, Oct. 1979, Abstr., p. 272.
14) M. Sano, Y. Hatano, and H. Yamatera, *Chem. Lett.*, **1979**, 789.